Journal of Advances in Engineering Sciences and Technology, 2025, 1(1), 35-54
https://doi.org/10.71204/85h4j926

Intelligent Vehicles Path Tracking Control Strategy Based on Sliding Mode Variable Weight MPC

Yiheng Shi [1], Qiangqiang Yao [1, *], Zhendong Zhu [1], Qilin Xie[1], Xingdong Sun [2, *]

[1] School of Mechanical Engineering, Qinghai University, Xining 810016, China

[2] Anhui Agricultural University, Hefei 230036, China

*** Correspondence:**

Qiangqiang Yao

yaoqiang@bjtu.edu.cn

Xingdong Sun

xdsun@ahau.edu.cn

Received: 28 May 2025/ Accepted: 27 October 2025/ Published online: 30 October 2025

Abstract

Traditional model predictive control (MPC) algorithms often suffer from slow trajectory convergence and non-smooth control increments when applied to complex driving scenarios. To address these challenges, this paper presents a novel trajectory tracking control method for intelligent vehicles based on sliding-mode variable-weight MPC. An adaptive variable-weight strategy is introduced within the MPC framework by integrating a sliding mode control (SMC) mechanism. This approach allows for real-time adjustment of the weight matrix in the MPC objective function based on the lateral displacement error and yaw angle error. This improves the controller's ability to adapt, enhances tracking precision, and ensures stability across different driving conditions. A vehicle dynamics model is constructed with front wheel steering angle as the control input, and the influence of different weighting coefficients on control performance is systematically analyzed. The proposed control strategy is implemented in Simulink and validated through co-simulation with a high-fidelity CarSim vehicle model under a double lane-change scenario. Simulation results show that, compared to conventional MPC, the proposed method reduces peak lateral displacement error by up to 71% and achieves notable improvements in yaw angle and lateral deviation of the vehicle's center of mass. These results demonstrate the effectiveness of the proposed approach in improving trajectory tracking performance, vehicle stability, and dynamic responsiveness.

Keywords: Model Predictive Control; Variable Weights; Sliding Mode Control; Trajectory Tracking

1. Introduction

Intelligent driving technology (Yu, 2016), as a frontier field of the deep integration of artificial intelligence and the automotive industry, is leading the strategic transformation of the global

automotive industry. With the development of high-end equipment such as intelligent manufacturing, automatic driving and intelligent robots (Li et al., 2024), higher requirements have been put forward for the precision, robustness and real-time performance of the motion control system. Trajectory tracking control, as the core enabling technology of intelligent driving system, directly determines the accuracy and reliability of vehicle motion control. Therefore, to achieve high-precision and high-robustness trajectory tracking control, the optimal design of control strategy becomes a key research direction.

The existing trajectory tracking control algorithms are mainly: there are PID control (Nuhel et al., 2023) LQR control (Peicheng et al., 2022), fuzzy control (Pareek et al., 2023), model predictive control (MPC) and so on (Wu et al., 2020). Model predictive control can realize multi-variable and multi-constraint rolling optimization, and it is robust to the disturbance of uncertain parameters (Tian et al., 2022), so it becomes a research hot spot in trajectory tracking control. In recent years, some scholars have improved the MPC trajectory tracking performance by combining two algorithms. Shi (2022) proposed a vehicle path tracking control method that combines an enhanced model predictive control (MPC) approach with PID theory (Shi et al., 2022). The lateral control incorporates a front wheel lateral deflection constraint and introduces a relaxation factor to maintain driving stability. Additionally, a PID controller is used for longitudinal control to adjust driving speeds according to varying road conditions (Yang et al., 2017). proposed a control strategy that balances vehicle speed response and trajectory tracking performance consisting of a trajectory planning module based on model predictive control and a dynamics control module based on direct adaptive fuzzy control. However, the multi-algorithm has certain requirements on the performance of the controller. An improved model predictive control method based on particle swarm optimization is developed, which can significantly reduce the total computational burden due to the seamless connection and mutual reinforcement between the two layers of optimization (Zuo et al., 2020). Alcalá (2019) based on cascade control, where the external loop solves the position control using the newly designed TS-MPC method, and the internal loop uses the TS-LMI-LQR algorithm designed through linear matrix inequalities to dynamically control the vehicle through secondary regulation, thus significantly reducing the computational time.

There are also scholars who, starting from the constraint. A robust model predictive control algorithm for the wheeled mobile robot tracking problem was proposed by Dai (2020) The robust tracking model predictive controller designed by considering the robot subjected to bounded disturbances and various practical constraints with the introduction of incremental input constraints. An adaptive learning model predictive control scheme was proposed by Zhang et al (2021), Wu et al (2020) employed model predictive control to develop a trajectory tracking controller, utilizing active steering and drive/brake, while accounting for actuator limitations and vehicle dynamic stability constraints.. In addition considering curvature is also a major hotspot. Tang et al (2020) proposed a controller design considering road curvature perturbation, uncertainty modeling error, and angle compensation based on the analysis of vehicle sideslip. However, all the above methods are controllers designed by considering specific factors under specific working conditions, which cannot meet the needs of multi-scenarios, so some scholars

turned to adaptive control. Liu et al (2023) introduced a two-layer model predictive control algorithm with curvature adaptation applied to path tracking for high-speed automated driving when encountering the problem of large trajectory curvature. Oh et al (2022) proposed an adaptive weighted prediction method based on a sliding mode observer and a gray predictive model weighting function for the problem of external disturbances affecting the performance of MPC controllers. Bujarbaruah et al (2020) proposed an adaptive MPC framework for uncertain linear systems. Yang et al (2017) proposed a control strategy that balances vehicle speed response and trajectory tracking performance consisting of a trajectory planning module based on model predictive control and a dynamics control module based on direct adaptive fuzzy control.

Variable weighting has become a hot research topic in recent years. M. Amir et al. applied two vehicle models with different complexity levels to MPC control, and switched the low-precision model to improve the computational efficiency under complex conditions, but the method also faced the problem of loss of precision and accuracy. Zhang et al (2019) improved MPC by adopting Laguerre function exponential weighting (LEMPC) design. A large number of optimization parameters in the long field of view are reduced by introducing the composition function of the fitted orthogonal sequence, thus significantly reducing the complexity without sacrificing the tracking accuracy (Tian et al., 2022), and a decreasing characteristic is also introduced to solve the problem of improving the robustness of the path controller (Tian et al., 2022). Some scholars have improved the computation rate by changing the sampling frequency (Xue et al., 2020) predicting the time domain (Funke et al., 2016), or parallel computation (Bai et al., 2019), but this method makes the control volume change roughly, and the accuracy and reliability of the control inputs are difficult to guarantee (Amer et al., 2017). Wang et al (2021) used the Mamdani fuzzy algorithm to regulate the transverse displacement objective weights of the MPC, which improves the controller's robustness to paths with different curvatures. robustness of the controller to paths with different curvatures. However, this method cannot meet the demand of MPC for fast response of the controller.

This paper introduces sliding mode control to achieve variable weight adaptive MPC control based on the lateral displacement error and yaw error of the vehicle's driving path. Using sliding mode control with fast dynamic response as an adaptive controller, coordinate the weight matrix of the changing objective function, and establish a two-degree-of-freedom vehicle dynamics model, sliding mode control is introduced on the basis of the MPC controller. By coordinating the weighting coefficients Q_Y, Q_φ, and $R_{\Delta\delta}$, which act on the lateral displacement, target yaw, and control increment, respectively, the accuracy and stability of trajectory tracking are improved in a coordinated manner, and the adaptability of trajectory tracking is enhanced.

2. Vehicle Dynamics Model

An accurate vehicle dynamics model is fundamental to the effectiveness of MPC. This study focuses on the trajectory tracking problem without delving into the detailed modeling of suspension characteristics. To enable the vehicle to follow the desired trajectory with greater accuracy and stability, the vehicle dynamics model is formulated based on Newton’s second law.

Specifically, the longitudinal dynamics along the x-axis, lateral dynamics along the y-axis, and yaw dynamics about the z-axis of the vehicle's center of mass are established.

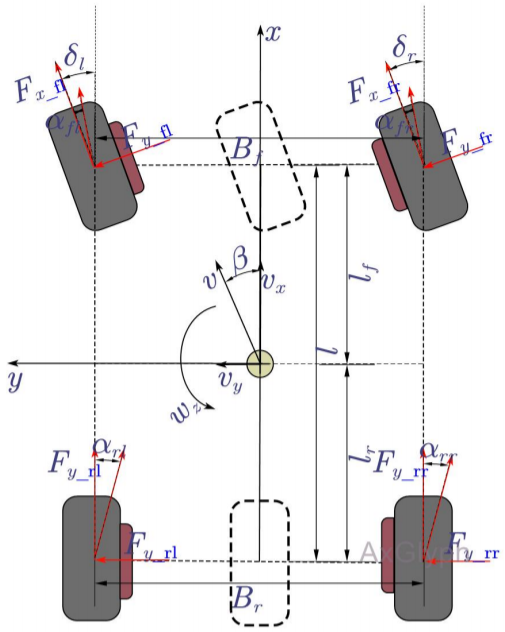

Figure 1. Schematic diagram of a vehicle planar motion model

Longitudinal dynamics of vehicle motion along the x-axis:

$$\sum F_x = m(\ddot{x} - \dot{y}\dot{\varphi}) = 2F_{xf} + 2F_{xr} \tag{1}$$

Transverse dynamics of vehicle motion along the y-axis:

$$\sum F_y = m(\ddot{y} + \dot{x}\dot{\varphi}) = 2F_{yf} + 2F_{yr} \tag{2}$$

Equations for the dynamics of the transverse pendulum of a vehicle rotating in the z-axis direction:

$$\sum M_z = I_z\ddot{\varphi} = 2aF_{yf} - 2bF_{yr} \tag{3}$$

Where, m is the mass of the vehicle; x is the longitudinal displacement of the vehicle and y is the lateral displacement of the vehicle; φ is the vehicle swing angle; I_z is the moment of inertia of the vehicle rotating around the z-axis; a represents the distance from the vehicle's center of mass to the front axle, while b denotes the distance to the rear axle. F_{xf} and F_{xr} are the longitudinal forces acting on the front and rear wheels along the x-axis, respectively, and F_{yf} and F_{yr} are the lateral forces on the front and rear wheels along the y-axis, respectively.

During the normal driving of the vehicle, the tire force is approximately described as a linear function and has a high fitting accuracy when the lateral acceleration is not greater than 0.4g. Therefore, the longitudinal force and the lateral deflection force of the tire are expressed by a linear relationship with the expression:

$$\begin{cases} F_{xf} = C_{lf} s_f \\ F_{xr} = C_{lr} s_r \end{cases} \tag{4}$$

$$\begin{cases} F_{yf} = -C_{cf}(\delta_f - \dfrac{y + a\dot{\varphi}}{\dot{x}}) \\ F_{yr} = -C_{cr}(\dfrac{b\dot{\varphi} - \dot{y}}{\dot{x}}) \end{cases} \tag{5}$$

Where, C_{lf} and C_{lr} are the longitudinal stiffness of the front and rear wheels, C_{cf} and C_{cr} are the lateral deflection stiffness of the front and rear wheels, s_f and s_r are the longitudinal slip rates of the front and rear wheels; and δ_f is the front wheel turning angle of the vehicle.

The transformation equation between the vehicle body coordinate system and the inertial coordinate system is:

$$\begin{cases} \dot{Y} = \dot{x}\sin\varphi + \dot{y}\cos\varphi \\ \dot{X} = \dot{x}\cos\varphi - \dot{y}\sin\varphi \end{cases} \tag{6}$$

From the above equations, based on the small angle assumption of the front wheels, the vehicle dynamics model can be simplified as follows.

$$\begin{aligned} \ddot{x} &= \dot{y}\dot{\varphi} + \frac{2}{m}\left(C_{\mathrm{lf}} s_{\mathrm{f}} + C_{\mathrm{cf}}(\delta_{\mathrm{f}} - \frac{\dot{y} + a\dot{\varphi}}{\dot{x}})\delta_{\mathrm{f}} + C_{\mathrm{lr}} s_{\mathrm{r}} \right) \\ \ddot{y} &= -\dot{x}\dot{\varphi} + \frac{2}{m}\left(C_{\mathrm{cf}}(\delta_{\mathrm{f}} - \frac{\dot{y} + a\dot{\varphi}}{\dot{x}}) + C_{\mathrm{cf}}(\frac{b\dot{\varphi} - \dot{y}}{\dot{x}}) \right) \\ \ddot{\varphi} &= \frac{2}{I_z}\left(aC_{\mathrm{cf}}(\delta_{\mathrm{f}} - \frac{\dot{y} + a\dot{\varphi}}{\dot{x}}) - bC_{\mathrm{cr}}(\frac{b\dot{\varphi} - \dot{y}}{\dot{x}}) \right) \\ \dot{\varphi} &= \dot{\varphi} \\ \dot{X} &= \dot{x}\cos\varphi - \dot{y}\sin\varphi \\ \dot{Y} &= \dot{x}\sin\varphi + \dot{y}\cos\varphi \end{aligned} \tag{7}$$

Then the state space equation of the system can be expressed as:

$$\begin{cases} \dot{\xi}(t) = f(\xi(t), \boldsymbol{u}(t)) \\ \eta = \boldsymbol{C}\xi(t) \end{cases} \tag{8}$$

Where the state vector is, the control input is $\xi = (\dot{x}, \dot{y}, \psi, \dot{\psi}, X, Y)^{\mathrm{T}}$, the front wheel angle $u=\delta_f$, and the system output is $\eta = (\psi, Y)$.

3. Model Predictive Control

3.1. Linearization and Discretization of the Model

The linearized model is obtained by using Taylor series expansion for the nonlinear model and neglecting the higher order terms to approximate the linearized model as follows:

$$\begin{cases} \dot{\xi} = f(\xi_r, u_r) + A(t)(\xi - \xi_r) + B(t)(u - u_r) \\ \eta = C(t)\xi \end{cases} \quad (9)$$

Where, $A(t) = \frac{\partial f}{\partial \xi}|_{\xi=\xi_r}$, $B(t) = \frac{\partial f}{\partial u}|_{u=u_r}$.

Write the first equation in incremental form:

$$\dot{\tilde{\xi}} = \tilde{\xi} - \tilde{\xi}_r = \frac{\partial f}{\partial \xi}|_{\substack{\xi=\xi_r \\ u=u_r}} \tilde{\xi} + \frac{\partial f}{\partial u}|_{\substack{\xi=\xi_r \\ u=u_r}} \tilde{u} \quad (10)$$

Using the forward Eulerian method, the discrete state space expression is obtained using the first order difference quotient instead of differentiation as:

$$\tilde{\xi}(k+1) = A(k)\tilde{\xi}(k) + B(k)\tilde{u}(k) \quad (11)$$

Where, $A(k)=I+TA(t)$; $B(k)=TB(t)$; I is the unit matrix; T is the sampling period of the model predictive controller; and k is the discrete step size.

$$x(k|t) = \begin{pmatrix} \xi(k|t) \\ u(k-1|t) \end{pmatrix} \quad (12)$$

Then the state space expression of the system is

$$\begin{cases} x(k+1|t) = \tilde{A}(k)x(k|t) + \tilde{B}(k)\Delta u(k|t) \\ y(k|t) = \tilde{C}(k)x(k|t) \end{cases} \quad (13)$$

Where, $\tilde{A}(k) = \begin{pmatrix} A(k) & B(k) \\ 0 & I \end{pmatrix}$ is the state equation; $\tilde{B}(k) = \begin{pmatrix} B(k) \\ I \end{pmatrix}$ is the control equation; and $\tilde{C}(k) = C$ is the output equation.

3.2. Constructing Prediction Equations

$$\begin{aligned} y(k+1|k) &= \tilde{C}\tilde{A}x(k|k) + \tilde{C}\tilde{B}\Delta u(k) \\ y(k+2|k) &= \tilde{C}\tilde{A}^2x(k|k) + \tilde{C}\tilde{A}\tilde{B}\Delta u(k) + \tilde{C}\tilde{B}\Delta u(k+1) \\ y(k+3|k) &= \tilde{C}\tilde{A}^3x(k|k) + \tilde{C}\tilde{A}^2\tilde{B}\Delta u(k) + \tilde{C}\tilde{A}\tilde{B}\Delta u(k+1) + \tilde{C}\tilde{B}\Delta u(k+2) \\ &\vdots \\ y(k+N_p|k) &= \tilde{C}\tilde{A}^{N_p}x(k|k) + \tilde{C}\tilde{A}^{N_p-1}\tilde{B}\Delta u(k) + \cdots + \tilde{C}\tilde{A}^{N_p-N_c}\tilde{B}\Delta u(k+N_c-1) \end{aligned} \quad (14)$$

Written in the form of a matrix:

$$Y(t) = \Psi(t)x(t) + \Theta(t)\Delta U(t) \quad (15)$$

Where， $Y(k)=\begin{pmatrix} y(k+1|k) \\ y(k+2|k) \\ \vdots \\ y(k+N_c|k) \\ \vdots \\ y(k+N_p|k) \end{pmatrix}$; $\Psi(k)=\begin{pmatrix} \tilde{C}(k)\tilde{A}(k) \\ \tilde{C}(k)\tilde{A}(k)^2 \\ \cdots \\ \tilde{C}(k)\tilde{A}(k)^{N_c} \\ \cdots \\ \tilde{C}(k)\tilde{A}(k)^{N_p} \end{pmatrix}$;

$$\boldsymbol{\Theta}(k)=\begin{pmatrix} \tilde{\boldsymbol{C}}(k)\tilde{\boldsymbol{B}}(k) & 0 & 0 & 0 \\ \tilde{\boldsymbol{C}}(k)\tilde{\boldsymbol{A}}(k)\tilde{\boldsymbol{B}}(k) & \tilde{\boldsymbol{C}}(k)\tilde{\boldsymbol{B}}(k) & 0 & 0 \\ \cdots & \cdots & \cdots & \\ \tilde{\boldsymbol{C}}(k)\tilde{\boldsymbol{A}}(k)^{N_c}\tilde{\boldsymbol{B}}(k) & \tilde{\boldsymbol{C}}(k)\tilde{\boldsymbol{A}}(k)^{N_c-1}\tilde{\boldsymbol{B}}(k) & \ldots & \tilde{\boldsymbol{C}}(k)\tilde{\boldsymbol{A}}(k)\tilde{\boldsymbol{B}}(k) \\ \vdots & \vdots & & \vdots \\ \tilde{\boldsymbol{C}}(k)\tilde{\boldsymbol{A}}(k)^{N_p-1}\tilde{\boldsymbol{B}}(k) & \tilde{\boldsymbol{C}}(k)\tilde{\boldsymbol{A}}(k)^{N_p-2}\tilde{\boldsymbol{B}}(k) & \ldots & \tilde{\boldsymbol{C}}(k)\tilde{\boldsymbol{A}}(k)^{N_p-N_c-1}\tilde{\boldsymbol{B}}(k) \end{pmatrix}.$$

3.3. Objective Function

The core of trajectory tracking control is to optimize an objective function to make the system run along a given trajectory as much as possible while satisfying a set of constraints. The objective function reflects the controller's desire to minimize the "cost" of tracking a given trajectory, and the objective function in this paper is designed as shown in equation (16).

$$J=\sum_{i=1}^{N_P} y\left(t+i|t\right)-y_{\text{ref}}\left(t+i|t\right)_Q^2+\sum_{i=0}^{N_c-1}\Delta u\left(t+i|t\right)_R^2+\rho\varepsilon^2 \tag{16}$$

The first part of the objective function reflects the trajectory tracking capability with the goal of minimizing the error between the predicted output and the reference output, i.e., the accuracy of trajectory tracking; the second part reflects the vehicle stabilization capability with the goal of minimizing the change of the front wheel angle of the control quantity, i.e., the stability of the trajectory tracking control increment, and the third part reflects the relaxation factor introduced to prevent the objective function from being unsolvable. Q is the system within the prediction time domain Np input weights, where Q_Y is the lateral displacement tracking target weights and Q_φ is the desired traverse tracking target weights; R is the control output weights within the prediction time domain Np.

$$Q=\begin{pmatrix} \begin{pmatrix} Q_\varphi & 0 \\ 0 & Q_Y \end{pmatrix}_1 & 0 & \cdots & 0 & \cdots & 0 \\ 0 & \begin{pmatrix} Q_\varphi & 0 \\ 0 & Q_Y \end{pmatrix}_2 & \cdots & 0 & \cdots & 0 \\ \vdots & \vdots & & \vdots & \vdots & \vdots \\ 0 & 0 & \cdots & \begin{pmatrix} Q_\varphi & 0 \\ 0 & Q_Y \end{pmatrix}_{N_c} & \cdots & 0 \\ \vdots & \vdots & \vdots & \vdots & & \vdots \\ 0 & 0 & \cdots & 0 & \cdots & \begin{pmatrix} Q_\varphi & 0 \\ 0 & Q_Y \end{pmatrix}_{N_p} \end{pmatrix} \tag{17}$$

$$\boldsymbol{R}=\begin{pmatrix}[R_{\Delta\delta}]_0 & 0 & \cdots & 0\\ 0 & [R_{\Delta\delta}]_1 & \cdots & 0\\ \vdots & \vdots & & \vdots\\ 0 & 0 & \cdots & [R_{\Delta\delta}]_{N_c-1}\end{pmatrix} \tag{18}$$

Quadratic programming has the advantages of being structured, efficient in solving, and robust in dealing with MPC problems, so quadratic programming is used to solve the trajectory tracking control problem in MPC. In addition, in order to make the controller both safe and feasible in real systems, therefore constraint design is introduced in the model predictive control.

$$\min_{\Delta U(t)} J=\min_{\Delta U(t)}\left\{\frac{1}{2}\begin{pmatrix}\Delta\boldsymbol{U}(t)\\ \boldsymbol{\varepsilon}\end{pmatrix}^{\mathrm{T}} H_t\begin{pmatrix}\Delta\boldsymbol{U}(t)\\ \boldsymbol{\varepsilon}\end{pmatrix}+G_t\begin{pmatrix}\Delta\boldsymbol{U}(t)\\ \boldsymbol{\varepsilon}\end{pmatrix}\right\} \tag{19}$$

Where, $\Delta U(t)=Y_t x(t\,|\,t)-\tilde{Y}_{\mathrm{ref}}(t)$; $\boldsymbol{G}_t=\begin{pmatrix}2\boldsymbol{E}(t)^{\mathrm{T}}\boldsymbol{Q}\boldsymbol{\Theta}_t & 0\end{pmatrix}$; $\boldsymbol{H}_t=2\begin{pmatrix}\left(\boldsymbol{\Theta}_t^{\mathrm{T}}\boldsymbol{Q}\boldsymbol{\Theta}_t+\boldsymbol{R}\right) & 0\\ 0 & \rho\end{pmatrix}$.

$$\begin{aligned}&\text{s.t. } \Delta U_{\min}\le\Delta U_t\le U_{\max}\\ &U_{\min}\Delta U_t+U_t \quad U_{\max}\\ &Y_{sc\min} \quad -\varepsilon Y_{sc}(t) \quad Y_{sc\max} \quad +\varepsilon\end{aligned} \tag{20}$$

Where, $A=\begin{pmatrix}1 & 0 & \cdots 0\\ 1 & 1 & \cdots 0\\ \vdots & \vdots & \ddots \vdots\\ 1 & 1 & 1 & 1\end{pmatrix}_{N_c\times N_c}$; $Y_{\mathrm{ref}}(t)=\left(y_{\mathrm{ref}}(t_1\,|\,t)\ldots y_{\mathrm{ref}}\left(t_{N_p}\,|\,t\right)\right)$.

Solving the above equation at each control cycle yields a sequence of control increments.

$$\Delta\boldsymbol{U}_t=\left(\Delta u_t,\Delta u_{t+1},\cdots,\Delta u_{t+N_c-1}\right)^{\mathrm{T}} \tag{21}$$

Use the first element of this sequence to get the optimal sequence for the current moment in time.

$$u(t)=u(t-1)+\Delta u_t \tag{22}$$

The front wheel angle obtained from the above optimization solution is input to the vehicle as the desired front wheel angle, and the next control cycle continues to repeat the above process, which can realize the trajectory tracking of the vehicle

4. Controller Design

4.1. Effect of Different Weight Coefficients on Performance

In order to balance the accuracy of trajectory tracking and system stability, and to enhance the adaptability to different working conditions, a sliding mode control algorithm is introduced into the designed MPC controller, so as to realize the adaptive variable weight control strategy. The weighting coefficients affecting the trajectory tracking performance are Q_Y, Q_φ, and $R_{\Delta\delta}$, which affect the lateral displacement, target traverse, and control increment of vehicle trajectory tracking, respectively.

In vehicle trajectory tracking control, the weight coefficient Q_Y regulates the lateral deviation between the current position of the vehicle and the reference trajectory. The effect of weight coefficient Q_Y on trajectory tracking performance is shown in Figure 2. In the figure, the weighting coefficient Q_φ is taken as 500 and the weighting coefficient $R_{\Delta\delta}$ is taken as 10000. it can be seen from the two figures that the weighting coefficient Q_Y has a significant effect on the vehicle trajectory tracking performance.

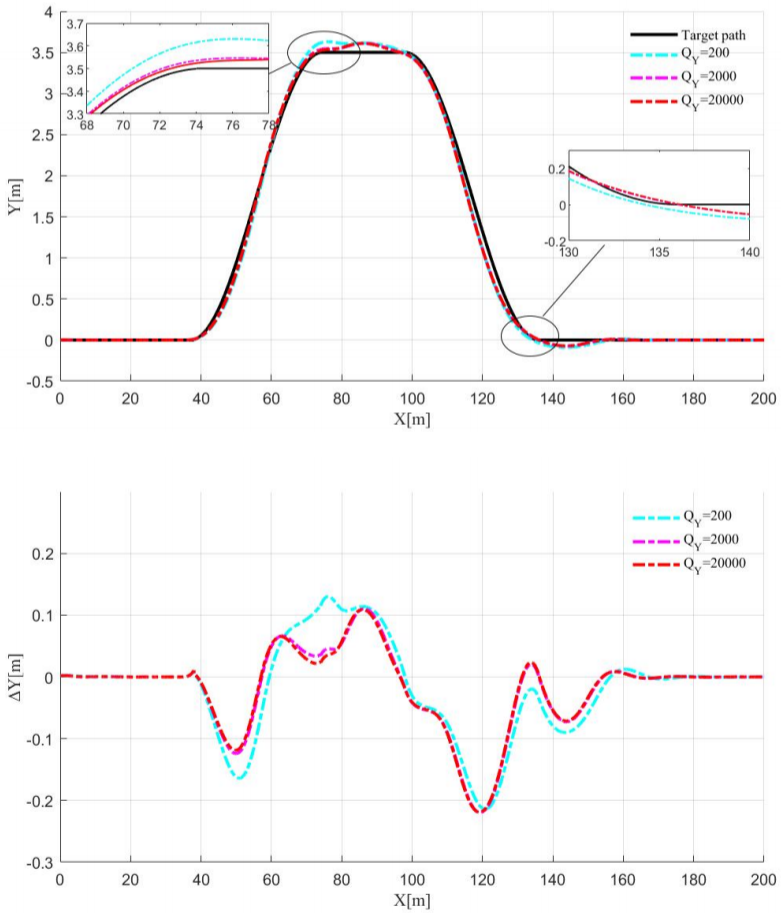

Figure 2. Q_Y Impact on trajectory tracking performance

In the trajectory tracking plots, Q_Y is taken as 200, 2000 and 20000, respectively. among them, Q_Y=2000 tracks closest to the target trajectory, and especially performs the best at key locations such as turns; while Q_Y=200 maintains better tracking despite a slight deviation; and Q_Y=20000 shows significant deviation, especially at the turns where the deviation is the largest. The lateral

error map shows that the Q_Y=2000 has the smallest lateral error fluctuation and converges quickly, with good system stability; the Q_Y=200 is also stable but with a slightly larger error; and the Q_Y=20000 shows stronger oscillation, with the largest error fluctuation and unstable control. In summary, Q_Y=2000 achieves the best balance between tracking accuracy, control smoothness and system stability, and has the best overall performance, but only changing Q_Y cannot meet the demand for trajectory tracking accuracy, so it needs to be changed in coordination with other parameters.

In the vehicle trajectory tracking control, the weight coefficient Q_φ is used to regulate the tracking accuracy of the vehicle target traverse angular velocity. The effect of the weight coefficient Q_φ on the trajectory tracking performance is shown in Figure 3. In the figure, the weighting coefficient Q_Y is taken as 1000 and the weighting coefficient $R_{\Delta\delta}$ is taken as 50000.From the two figures, it can be seen that the weighting coefficient Q_φ has a significant effect on the dynamic response and the stability of the traverse angle of the vehicle trajectory tracking.

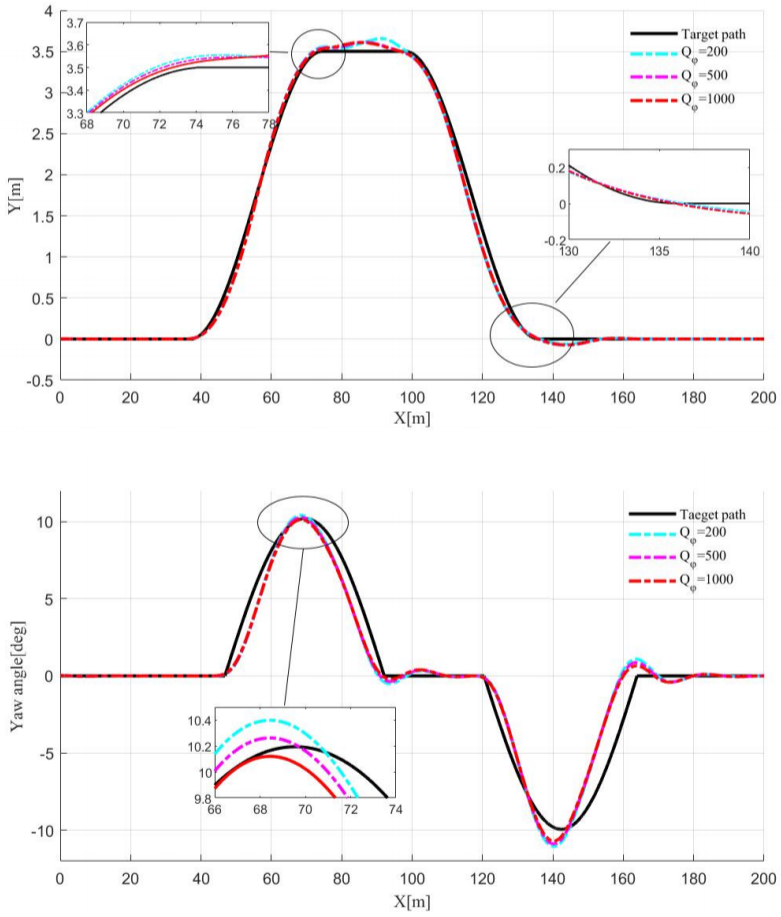

Figure 3. Q_φ Impact on trajectory tracking performance

From the Figure 3, it can be seen that the traverse angle error weight Q_φ has a significant effect on the trajectory tracking performance. In the transverse position plot, as Q_φ is increased from 100 to 1000, the tracking accuracy of the vehicle at the turn is significantly improved, especially when the trajectory almost completely fits the target path at Q_φ=1000. In the transverse swing angle

diagram, the fluctuation is larger when Q_φ = 100; the control effect is improved when Q_φ = 500; and the contrasting Q_φ = 1000 curve shows higher attitude stability and smaller fluctuation.

Comprehensive analysis shows that appropriately increasing Q_φ can effectively improve the turning accuracy, while reasonably setting Q_Y can help stabilize the pendulum angle control, and the trade-off between the two can achieve better trajectory tracking performance.

In vehicle trajectory tracking control, the weighting coefficient $R_{\Delta\delta}$ is used to regulate the magnitude of change in the steering control increments, which affects the smoothness of the control inputs. The effect of the weighting coefficient $R_{\Delta\delta}$ on the trajectory tracking performance is shown in Figure.4 . In the figure, the weight coefficient Q_Y is taken as 1000 and the weight coefficient Q_φ is taken as 500.From the figure, it can be seen that the weight coefficient $R_{\Delta\delta}$ has a significant effect on the smoothness and response speed of the control system.

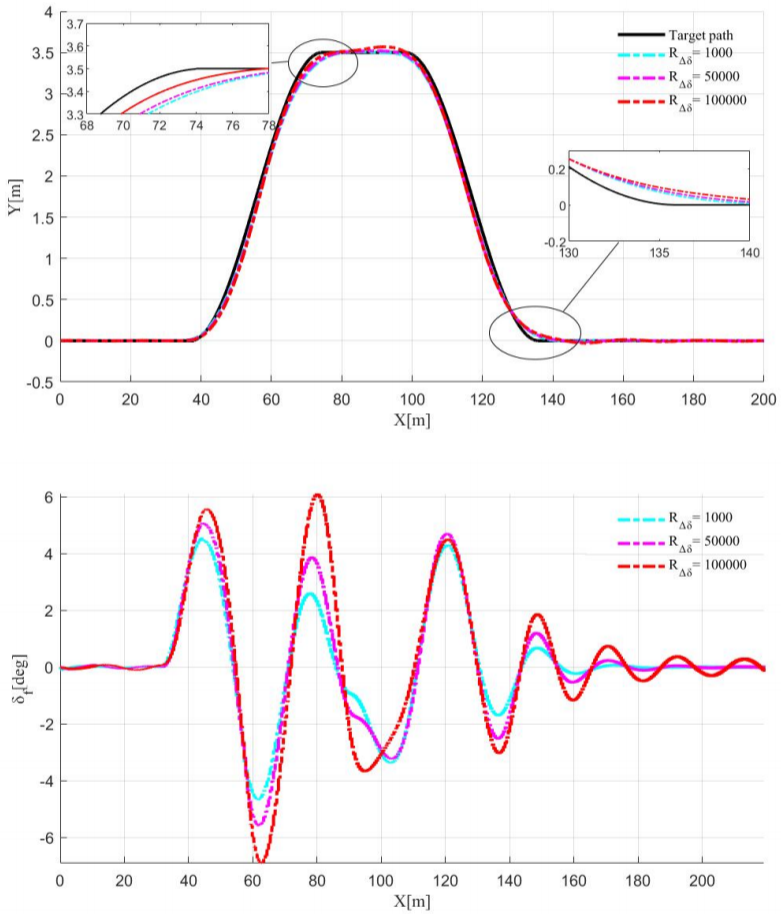

Figure 4. $R_{\Delta\delta}$ Impact on trajectory tracking performance

From the Figure 4, it can be seen that the control incremental weight $R_{\Delta\delta}$ has a significant effect on the trajectory tracking performance and control smoothness. With the increase of $R_{\Delta\delta}$, the change amplitude of the front wheel corner of the vehicle gradually decreases, and the control tends to be smooth, but the trajectory tracking accuracy decreases subsequently. When $R_{\Delta\delta}$ = 1000, the vehicle trajectory is closest to the target path, and the corner response is sensitive but fluctuates greatly; when $R_{\Delta\delta}$=10000, the control smoothness is improved, and the tracking accuracy is slightly reduced; and when $R_{\Delta\delta}$ is increased to 100000, the control action is the smoothest, and the change of the front wheel angle is the smallest, but the cornering section is

obviously deviated from the target trajectory. It can be seen that a smaller $R_{\Delta\delta}$ is more conducive to improving the trajectory tracking accuracy, while a larger $R_{\Delta\delta}$ helps to improve the control smoothness, which should be set according to the actual needs of the system for trade-off.

4.2. Sliding Mode Surface Design and Dynamic Weight Adjustment Strategy

Combined with the above analysis, choosing different weighting parameters control system has different effects on the error of trajectory tracking. Therefore, the effects of the three key weighting coefficients are considered comprehensively in the design of the sliding mode variable weight MPC controller.

(1) Sliding mold surface design

Transverse error slide mold surface design

$$s_Y = e_Y + \lambda_{Y1}\int_0^t e_Y(\tau)d\tau + \lambda_{Y2}\dot{e}_Y \tag{23}$$

Where, e_Y is the transverse error, the integral term $\int_0^t e_Y(\tau)d\tau$ is for eliminating the steady state error and solving the static difference of the system; the differential term $\dot{e}_Y$ is for suppressing the overshoot and enhancing the dynamic response of the system; and, λ_{Y1} and λ_{Y2} are the coefficients.

Transverse Pendulum Angle Error Sliding Mode Surface Design

$$s_\varphi = e_\varphi + \lambda_\varphi \dot{e}_\varphi \tag{24}$$

Where, e_φ is the pendulum angle error; λ_φ usually taken as 2.

(2) Dynamic weighting function

The lateral displacement weight Q_Y adjustment strategy with the following adjustment function:

$$Q_Y = Q_{Y0}\cdot\left(1+\alpha_Y\cdot\mathrm{sat}\left(\frac{|s_Y|}{\sigma_Y}\right)\right) \tag{25}$$

Where lateral displacement basis weights $Q_{Y0}=500$; regulation gain $\alpha_Y=1.6$; saturation threshold $\sigma_Y=0.15$, which corresponds to the tolerance of the lateral error; and normalization function.

The realization mechanism is that, $|s_Y|<\sigma_Y, Q_Y\approx Q_{Y0}$, the controller maintains the normal tracking state, and $|s_Y|\geq\sigma_Y$, the controller starts to strengthen the lateral control.

The transverse pendulum angle weights Q_φ adjustment strategy with the following adjustment function

$$Q_\varphi = Q_{\varphi 0}\cdot\exp\left(\beta_\varphi\cdot|s_\varphi|\right) \tag{26}$$

Where the transverse pendulum angle basis weights $Q_{\varphi 0}=1000$; the parameter $\beta_\varphi=0.6$.

The realization mechanism is, when $|s_\phi|<0.1$, is small error, smooth adjustment. Fast response when large error.

Controls incremental weight adjustments with the following adjustment function

$$R_{\Delta\delta}=\frac{R_0}{1+\gamma\cdot\sqrt{s_Y^2+s_\delta^2}} \tag{27}$$

Where, $R_0=10000$ and $\gamma=0.8$.

The regulation mechanism is to use a low sliding modulus for normal tracking, thus limiting control jitter, and a high sliding modulus for emergency corrective action, thus permitting greater steering rates.

4.3. Sliding Mode Variable Weight MPC Controller

When both the lateral displacement and swing angle errors are small, the vehicle traveling stability is strong, so Q_Y can be increased, and Q_φ, $R_{\Delta\delta}$ can be decreased to enhance the accuracy of trajectory tracking; when the lateral displacement and swing angle errors are large, the vehicle traveling stability is weak, so Q_Y can be decreased, and Q_φ, $R_{\Delta\delta}$ can be increased to enhance the tracking capability of the desired swing angle. Accurate tracking of the trajectory is achieved through Figure 5.

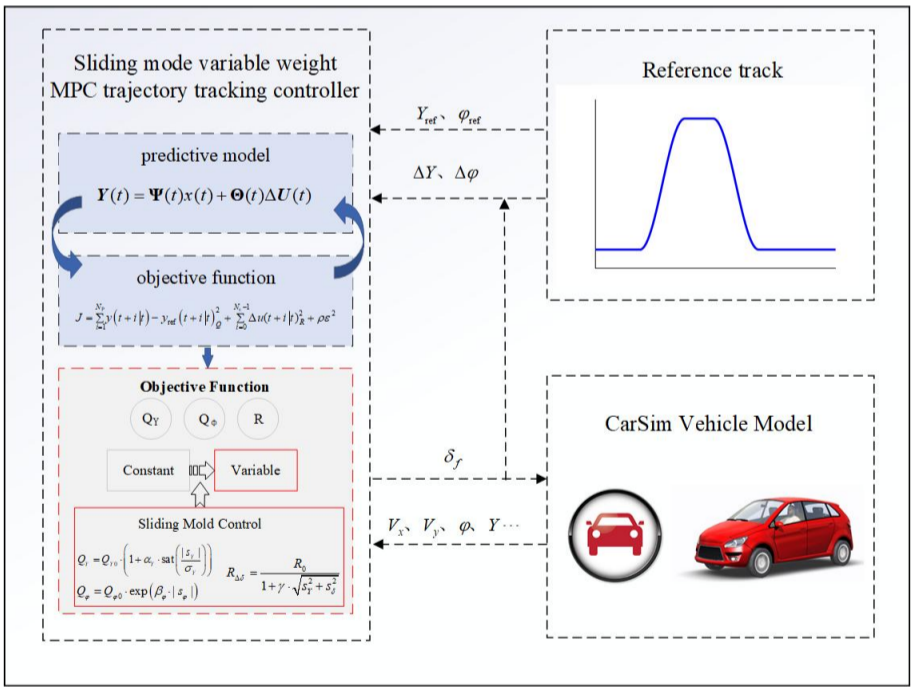

Figure 5. Carsim/Simulink sliding mode variable weight MPC trajectory tracking flowchart

5. Simulation Analysis

To validate the effectiveness of the aforementioned controller, trajectory tracking control was tested using Carsim/Simulink co-simulation. This approach was compared with the traditional MPC control described in References (Yang et al., 2024) to examine the impact of variable

weights on MPC trajectory tracking performance. The double-shift line condition is selected for simulation, and the vehicle speed is set as variable speed, that is, to realize the simulation of two-lane overtaking. The vehicle model parameters are shown in the following Table 1.The reference trajectory is shown in Figure 6.

Table 1. Main parameters of the car

parameters	value	clarification
m/kg	1650	Vehicle quality
l_f/m	1.400	Distance from front axle to the center of mass
l_r/m	1.650	Distance from front axle to the center of mass
I_z/(kg·m^2)	3234	Vehicle yaw inertia
h_{CG}/m	0.53	Center of gravity
D_f/m	1.58	Front axle width
D_r/m	1.58	Rear axle width

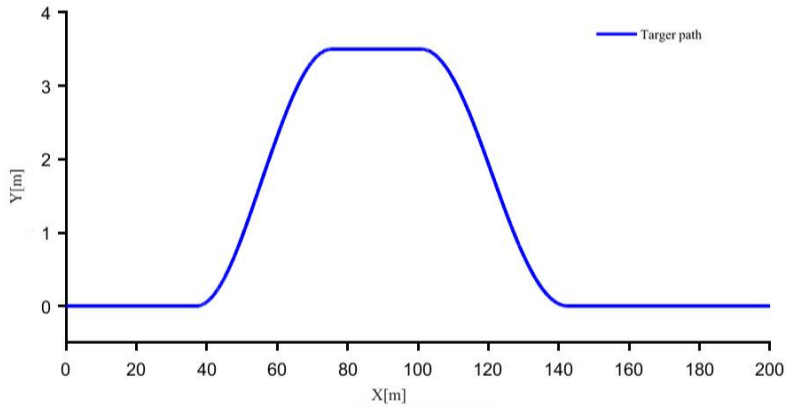

Figure 6. Target path

The transverse displacement map and the transverse displacement error map are shown in the following Figure 7 and Figure 8. From the transverse displacement map, both trajectories are very close to the target trajectory, which indicates that both controllers are able to fulfill the trajectory tracking task better. However, it can be clearly seen in the zoomed-in graph that the ordinary MPC (blue line) shows more obvious trajectory deviation in the region of large curvature change; while the variable weight MPC (red line) is closer to the target trajectory and shows stronger tracking ability in the curved segment. From the lateral displacement error diagram, it can be seen that the MPC controller shows large error fluctuations in several segments, especially in the position with obvious curvature changes (e.g., about X = 140), where the maximum error is close to ±0.3 m. The error fluctuations of the variable-weight MPC are obviously reduced, and the overall curve is smoother and with smaller error, showing stronger control accuracy and stability.

It shows that the improved control strategy can effectively suppress the lateral deviation and improve the robustness and tracking performance of the system.

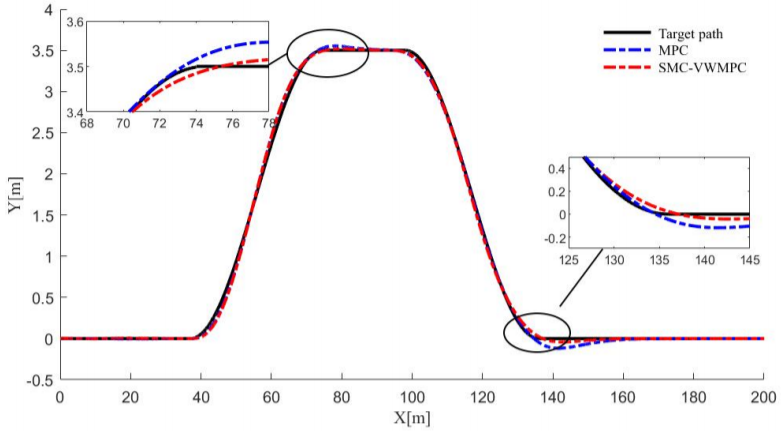

Figure 7. Trajectory tracking lateral displacement

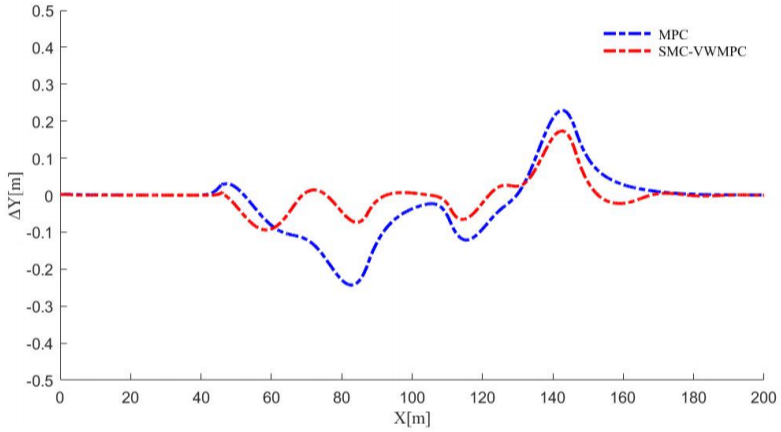

Figure 8. Trajectory tracking lateral error

Table 2. Peak Transverse Displacement Error

Peak point longitudinal position X/m	Peak point lateral position Y/m（MPC）	Peak point lateral position Y/m（SMC-VWMPC）	Optimization effect (%)
X=82.63	-0.24	-0.07	71
X=142.64	0.23	0.17	26

The trajectory tracking traverse angle is shown in Figure 9, from the overall point of view, the three curves are basically consistent in the overall trend, indicating that both the traditional MPC and the variable weight MPC can track the target traverse angle better. However, from the left local zoomed-in figure, it can be clearly seen that the traditional MPC controller has obvious hysteresis and has a large overshoot near the target angle, while the variable weight MPC responds faster, with smaller overshoot, and enters the stabilization zone earlier, which shows better control accuracy and dynamic response capability. As can be seen from the local zoomed-in

figure on the left side, the lowest point of the cross-swing angle of the normal MPC (i.e., the most drastic point of the cornering angle) deviates from the target curve and recovers slowly, while the variable-weighted MPC is closer to the target at the extreme point, with smaller fluctuations, and can return to the vicinity of the desired value faster, which embodies a stronger stability and robustness.

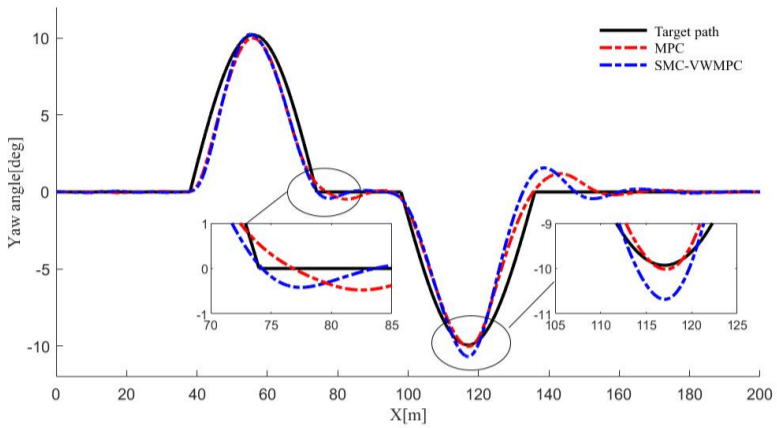

Figure 9. Trajectory tracking traverse angle

The trajectory tracking center-of-mass side deflection angle is shown in Figure 10, in which the side deflection angle fluctuates positively and negatively for many times in different road sections, reflecting the dynamic response of the vehicle in the process of turning and righting; the variable-weight MPC has the same trend of the trajectory tracking center-of-mass side deflection angle as that of the MPC controller, but there are many subtle differences, especially in the extreme value and the transition section. In the 40-60 m, 80-100 m and 110-130 m intervals, the peak value (maximum lateral deviation angle) of the normal MPC curve is significantly higher than that of the variable-weight MPC, which implies that the normal MPC has a larger lateral deviation angle and a more serious vehicle attitude deviation in large curvature turns, while the peak value of the red line is lower, The lower peak value and faster recovery of the red line indicate that the variable weight MPC can effectively suppress the drastic sideslip tendency and improve the attitude stability.

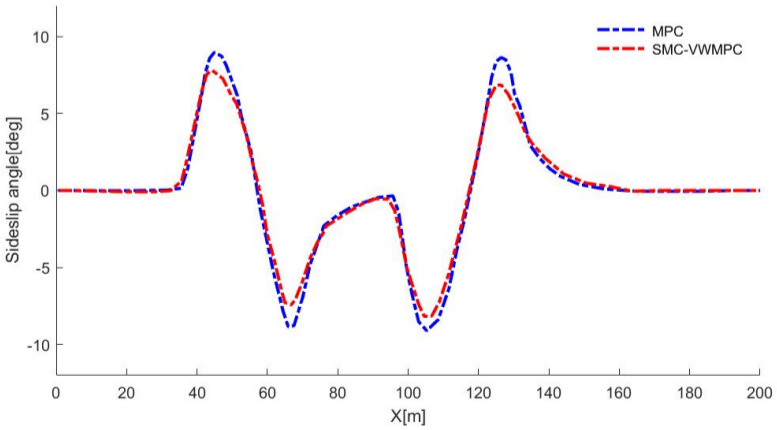

Figure 10. Trajectory tracking center-of-mass lateral declination

Based on controller processing time comparisons, this paper demonstrates that the adaptive sliding-mode variable-weight controller averages 16ms per operation but can reach up to 23ms during peak loads. This represents a 1.3-fold increase in computation time compared to conventional MPC controllers, indicating insufficient processor computational capacity under such conditions. Consequently, real-time performance can be enhanced by optimizing algorithmic structures or upgrading processor capabilities.

6. Conclusion

In this paper, a sliding mode variable weight MPC trajectory tracking control algorithm is proposed, and a joint simulation platform of Carsim and Simulink is constructed to verify the effectiveness of the variable weight MPC algorithm in trajectory tracking control. Compared with the traditional MPC control algorithm, the proposed control strategy shows good dynamic performance and robustness in terms of improving trajectory tracking accuracy, pendulum angular response, and the center-of-mass lateral deflection angle control. Robustness.

(1) The control system realizes good accuracy control in lateral displacement tracking. The transverse displacement error fluctuation is small, and the error peak value is significantly lower than that of the traditional method, which indicates that the system has strong anti-interference ability and accurate path fitting ability.

(2) As for the control of transverse swing angle and center of mass lateral deviation angle, the proposed algorithm maintains the stability and rapidity of the angular response, effectively suppresses the attitude deviation of the vehicle during dynamic lane changing or turning, and helps to improve the overall lateral stability of the vehicle.

(3) From the comparison of peak errors, the performance of the proposed algorithm improves significantly in several key indexes. Compared with the traditional control strategy, the maximum value of lateral displacement error is reduced by 71%, which verifies the adaptability and superiority of this control algorithm under high-speed and high-dynamic working conditions.

Author Contributions:

Conceptualization, Yiheng Shi. and Zhendong Zhu.; methodology, Yiheng Shi.; software, Yiheng Shi.; validation, Yiheng Shi.; formal analysis, Yiheng Shi.; data curation, Yiheng Shi.and Qilin Xie.; writing—original draft preparation, Yiheng Shi.and Xingdong Sun.; writing—review and editing, Yiheng Shi. and Qiangqiang Yao.; funding acquisition, Qiangqiang Yao. All authors have read and agreed to the published version of the manuscript.

Funding:

This work was supported in part by the Qinghai University Youth Research Fund, China (Grant No. 2023-QGY-15).

Data Availability Statement:

Because some of the data in this paper is part of an ongoing study, the dataset presented in the paper is not readily available.

Acknowledgments:

I am very grateful to my supervisor, Dr. Qiangqiang Yao, for his careful guidance on the dissertation, and to my fellow student, Zhendong Zhu, for his help on the dissertation ideas.

Conflict of Interest:

The authors declare no conflict of interest.

References

Alcalá, E., Puig, V., & Quevedo, J. (2019). TS-MPC for autonomous vehicles including a TS-MHE-UIO estimator. IEEE Transactions on Vehicular Technology, 68(7), 6403-6413.

Amer, N. H., Zamzuri, H., Hudha, K., & Kadir, Z. A. (2017). Modelling and control strategies in path tracking control for autonomous ground vehicles: A review of state of the art and challenges. Journal of intelligent & robotic systems, 86, 225-254.

Amir, M., & Givargis, T. (2017, November). Hybrid state machine model for fast model predictive control: Application to path tracking. In 2017 IEEE/Acm International Conference on Computer-Aided Design (Iccad) (pp. 185-192). IEEE.

Bai, G., Meng, Y., Liu, L., Luo, W., Gu, Q., & Li, K. (2019). A new path tracking method based on multilayer model predictive control. Applied sciences, 9(13), 2649.

Bujarbaruah, M., Nair, S. H., & Borrelli, F. (2020, May). A semi-definite programming approach to robust adaptive MPC under state dependent uncertainty. In 2020 European Control Conference (ECC) (pp. 960-965). IEEE.

Dai, L., Lu, Y., Xie, H., Sun, Z., & Xia, Y. (2020). Robust tracking model predictive control with quadratic robustness constraint for mobile robots with incremental input constraints. IEEE Transactions on Industrial Electronics, 68(10), 9789-9799.

Funke, J., Brown, M., Erlien, S. M., & Gerdes, J. C. (2016). Collision avoidance and stabilization for autonomous vehicles in emergency scenarios. IEEE Transactions on Control Systems Technology, 25(4), 1204-1216.

Li, X., Gong, X., Chen, Y. H., Huang, J., & Zhong, Z. (2024). Integrated path planning-control design for autonomous vehicles in intelligent transportation systems: A neural-activation approach. IEEE Transactions on Intelligent Transportation Systems, 25(7), 7602-7618.

Liu, H., Sun, J., & Cheng, K. W. E. (2023). A two-layer model predictive path-tracking control with curvature adaptive method for high-speed autonomous driving. IEEE access, 11, 89228-89239.

Nuhel, A. K., Al Amin, M., Paul, D., Bhatia, D., Paul, R., & Sazid, M. M. (2023, August). Model Predictive Control (MPC) and Proportional Integral Derivative Control (PID) for Autonomous Lane Keeping Maneuvers: A Comparative Study of Their Efficacy and

Stability. In International Conference on Cognitive Computing and Cyber Physical Systems (pp. 107-121). Cham: Springer Nature Switzerland.

Oh, K., & Seo, J. (2022). Development of an adaptive and weighted model predictive control algorithm for autonomous driving with disturbance estimation and grey prediction. IEEE Access, 10, 35251-35264.

Pareek, S., Gupta, H., Kaur, J., Kumar, R., & Chohan, J. S. (2023, June). Fuzzy logic in computer technology: Applications and advancements. In 2023 3rd International Conference on Pervasive Computing and Social Networking (ICPCSN) (pp. 1634-1637). IEEE.

Peicheng, S., Li, L., Ni, X., & Yang, A. (2022). Intelligent vehicle path tracking control based on improved MPC and hybrid PID. IEEE Access, 10, 94133-94144.

Tang, L., Yan, F., Zou, B., Wang, K., & Lv, C. (2020). An improved kinematic model predictive control for high-speed path tracking of autonomous vehicles. IEEE Access, 8, 51400-51413.

Tian, Y., Yao, Q., Hang, P., & Wang, S. (2022). A gain-scheduled robust controller for autonomous vehicles path tracking based on LPV system with MPC and H_∞. IEEE Transactions on vehicular technology, 71(9), 9350-9362.

Tian, Y., Yao, Q., Wang, C., Wang, S., Liu, J., & Wang, Q. (2022). Switched model predictive controller for path tracking of autonomous vehicle considering rollover stability. Vehicle system dynamics, 60(12), 4166-4185.

Wang, J., Teng, F., Li, J., Zang, L., Fan, T., Zhang, J., & Wang, X. (2021). Intelligent vehicle lane change trajectory control algorithm based on weight coefficient adaptive adjustment. Advances in Mechanical Engineering, 13(3), 16878140211003393.

Wu, H., Si, Z., & Li, Z. (2020). Trajectory tracking control for four-wheel independent drive intelligent vehicle based on model predictive control. IEEE Access, 8, 73071-73081.

Xue, W., & Zheng, L. (2020). Active collision avoidance system design based on model predictive control with varying sampling time. Automotive innovation, 3(1), 62-72.

Yang Z, Li S, Wang Z. Trajectory Tracking Control of Distributed Driving Intelligent Vehicles Based on Adaptive Variable Parameter MPC. Journal of Mechanical Engineering, 2024, 60(6): 363-377.

Yang, L., Yue, M., Ma, T., & Hou, X. (2017, July). Trajectory tracking control for 4WD vehicles using MPC and adaptive fuzzy control. In 2017 36th Chinese Control Conference (CCC) (pp. 9367-9372). IEEE.

Yu, F. R. (2016). Connected vehicles for intelligent transportation systems [guest editorial]. IEEE Transactions on Vehicular Technology, 65(6), 3843-3844.

Zhang, B., Zong, C., Chen, G., & Zhang, B. (2019). Electrical vehicle path tracking based model predictive control with a Laguerre function and exponential weight. IEEE Access, 7, 17082-17097.

Zhang, K., Sun, Q., & Shi, Y. (2021). Trajectory tracking control of autonomous ground vehicles using adaptive learning MPC. IEEE Transactions on Neural Networks and Learning Systems, 32(12), 5554-5564.

Zuo, Z., Yang, X., Li, Z., Wang, Y., Han, Q., Wang, L., & Luo, X. (2020). MPC-based cooperative control strategy of path planning and trajectory tracking for intelligent vehicles. IEEE Transactions on Intelligent Vehicles, 6(3), 513-522.